A Tokamak Engineering Test Reactor

R.W. Conn and D.L. Jassby

March 1975

UWFDM-119

FUSION TECHNOLOGY INSTITUTE

UNIVERSITY OF WISCONSIN

MADISON WISCONSIN

A Tokamak Engineering Test Reactor

R.W. Conn and D.L. Jassby

Fusion Technology Institute
University of Wisconsin
1500 Engineering Drive
Madison, WI 53706

http://fti.neep.wisc.edu

March 1975

UWFDM-119

A TOKAMAK ENGINEERING TEST REACTOR

R. W. Conn

Nuclear Engineering Department, University of Wisconsin
Madison, Wisconsin 53706

and

D. L. Jassby

Plasma Physics Laboratory, Princeton University
Princeton, New Jersey 08540

July 1975

MATT - 1155
FDM - 119 (revised)

Presented at International Conference on Radiation Test Facilities for the CTR Surface and Materials Program, July 15-18, 1975, Argonne National Laboratory, Argonne, Illinois, USA (to be published in Conference Proceedings).

A TOKAMAK ENGINEERING TEST REACTOR

R. W. Conn

Nuclear Engineering Department, University of Wisconsin
Madison, Wisconsin 53706

and

D. L. Jassby

Plasma Physics Laboratory, Princeton University
Princeton, New Jersey 08540

ABSTRACT

The design criteria for a tokamak engineering test reactor can be met by operating in the two-component mode with reacting ion beams, together with a new blanket-shield design based on internal neutron spectrum shaping. A conceptual reactor design achieving a neutron wall loading of about 1 MW/m^2 is presented. The tokamak has a major radius of 3.05 m, the plasma cross-section is noncircular with a 2:1 elongation, and the plasma radius in the midplane is 55 cm. The total wall area is 149 m^2. The plasma conditions are $T_e \simeq T_i \simeq 5$ keV, and $n\tau \simeq 8 \times 10^{12}$ $cm^{-3}s$. The plasma temperature is maintained by injection of 177 MW of 200-keV neutral deuterium beams; the resulting deuterons undergo fusion reactions with the triton-target ions. The D-shaped toroidal field coils are extended out to large major radius (7.0 m), so that the blanket-shield test modules on the outer portion of the torus can be easily removed. The TF coils are superconducting, using a cryogenically stable TiNb design that permits a field at the coil of 80 kG and an axial field of 38 kG. The blanket-shield design for the inner portion of the torus nearest the machine center line utilizes a neutron spectral shifter so that the first structural wall behind the spectral shifter zone can withstand radiation damage for the reactor lifetime. The energy attenuation in this inner blanket is 8×10^{-6}. If necessary, a tritium breeding ratio of 0.8 can be achieved using liquid lithium cooling in the outer blanket only. The overall power consumption of the reactor is about 340 MW(e). A neutron wall loading greater than 1 MW/m^2 can be achieved by increasing the maximum magnetic field or the plasma elongation.

1. INTRODUCTION

The engineering difficulties associated with the construction and operation of Tokamaks as fusion power reactors have been investigated in considerable detail in several recent conceptual Tokamak reactor design studies [1-3]. Whether the reactor is a pure fusion device using D-T fuel or a fission-fusion hybrid, these engineering problems include radiation damage to the reactor structural materials, blanket design for power conversion and breeding fuel (with all the inherent thermal hydraulics problems,) remote maintenance and handling, tritium leakage control, large bore toroidal field magnet design, and so on.

With these problems in mind, it becomes clear that a Tokamak engineering test reactor will be an integral part of any national or international program to achieve viable Tokamak fusion power reactors. The functions of such a reactor include testing blanket and shield designs, performing radiation damage and materials studies, and testing solutions to other major engineering problems, such as tritium handling and leakage control, and remote handling techniques. On the other hand, a reactor designed with these goals in mind need not have as one of its primary functions the generation of net electrical power.

The design goals for achieving the stated purposes of such a reactor are; (a) that the 14 MeV neutron wall loading should be about 1 MW/m^2 (to achieve the proper volumetric heating and bulk radiation damage); (b) that the surface heat load on the first wall be similar to that expected in Tokamak power reactors (to simulate first wall stresses and surface damage correctly); and (c) that sufficient space be available for blanket module design testing (such as the thermal hydraulics of particular blanket designs.) The test reactor should achieve these goals subject to the constraint that it be small, flexible, and as inexpensive as possible.

Recently, the design of a facility referred to as a FERF (for fusion engineering research facility) has been considered, with designs based on mirror confinement [4] or theta pinch confinement [5]. In particular, the mirror FERF design operating with an $n\tau$ three times less than classical has the merit of small size and should produce steady-state 14-MeV neutron fluxes at a level adequate for bulk radiation damage studies. On the other hand, the surface heat load will not simulate the charged particle, neutral, and radiation fluxes in Tokamaks, and the approximately 1 m^2 of test area will make extensive blanket and shield engineering tests difficult. Perhaps a small mirror FERF with more limited objectives will be the predecessor of a Tokamak engineering test reactor. On the other hand, if a Tokamak can perform the required functions, it will have certain inherent advantages. Three of these are especially important. First, it will simultaneously produce the most relevant first wall surface damage together with the correct bulk radiation damage. Second, it would automatically test other tokamak technologies, such as large bore superconducting toroidal field coils, which must be developed in any case. Third, because of its geometry, a Tokamak reactor necessarily has a large test area so that its cost, measured in dollars per square meter of test area, will surely be favorable. Therefore, extensive blanket and shield engineering tests as well as materials and radiation damage tests can be carried out.

In this paper, we examine the potential of a beam driven tokamak operating in the two-energy-component tokamak (TCT) mode [6,7] as a viable tokamak engineering test reactor. The TCT concept is combined with some recent innovations in blanket [8] and toroidal field magnet [9] design to produce a relatively small and flexible reactor which appears able to achieve the stated purposes. The remainder of the paper is structured as follows. In Section 2, we analyze the expected plasma behavior and, together with some of the design constraints, evolve a base-case tokamak engineering reactor design. In Section 3 and 4, the design of the blanket-shield and toroidal field coils are described. Particular emphasis is placed on the flexibility these design ideas bring to this reactor. In Section 5, we investigate the power requirements for such a reactor and present a rough cost estimate. Section 6 contains a study of alternative assumptions regarding magnetic field and plasma shape.

2. PLASMA AND MACHINE PARAMETERS

2.1 Scaling of Fusion Power Density

The fusion core of an engineering test reactor should have the maximum possible fusion power density, P_f. This section contains a discussion of the plasma conditions for maximizing P_f in a beam-driven tokamak reactor, and applies these results to determine suitable plasma parameters for such a reactor.

In a two-energy-component tokamak (TCT), the temperature of the tritium bulk plasma is maintained against transport and radiation losses by means of injected energetic deuterons, which undergo fusion reactions with the relatively cold tritons. The large beam-plasma fusion reactivity allows the TCT to attain a fusion energy gain, Q, approximately equal to 1 at values of $n\tau$ many times lower than that required for a Q=1 thermonuclear reactor (where all reacting ions are thermalized) [6]. The fusion energy gained is defined as

$$Q = \frac{\text{Fusion power produced by the plasma in neutrons and alphas}}{\text{Neutral beam power injected into the plasma}} \qquad (1)$$

No account is taken of any energy amplification by the blanket, so that the energy released per fusion reaction is 17.6 MeV. For driven tokamaks with the temperature maintained entirely by injected beams, we define

$$\bar{\Gamma} = (\text{fast-ion pressure/bulk-plasma pressure}) \simeq 0.5\tau_s/\tau_E \qquad (2)$$

where τ_s is the fast-ion slowing-down time, and τ_E is the bulk-plasma energy confinement time. For Q-values larger than attainable in "pure" TCT operation, $n_e\tau_E$ must be increased so that the injected beam power can be reduced while the proportion of the fusion power output coming from thermal-plasma reactions increases. At the same time, P_f decreases because of the reduction in beam-plasma reactions [7]. Therefore, attaining large Q requires thermal-plasma operation with large $n_e\tau_E$, while producing the largest neutron flux

demands TCT operation at low $n_e \tau_E$. The trade-off between Q and P_f for a given plasma pressure is shown in Fig. 1, taken from Ref. [7]. For a Tokamak engineering test reactor, a small-$n\tau$ plasma that delivers a large neutron flux at $Q \sim 1$ is desirable. As such, TCT operation is the optimal mode.

For given values of electron temperature, T_e, and injection energy, W_o, one can express P_f in terms of a single variable (for example, $\bar{\Gamma}$) which is then optimized to maximize P_f. The optimal values of $\bar{\Gamma}$ for W_o = 200 keV and the corresponding Q and P_f are shown in Fig. 2, as well as the maximum P_f for a thermonuclear reactor of the same pressure. At the conditions giving Q approximately equal to one in a TCT, P_f is a factor of four larger than the maximum P_f attainable in a thermal plasma at any temperature, for the same total plasma pressure.

For plasmas of arbitrary q, A=R/a, $\beta_\rho < A$, and axial magnetic field, B_t (in kG), the maximum attainable P_f is

$$P_f = 7.7 \times 10^{-5} P_{fo} \left(\frac{B_t}{qA}\right)^4 \beta_\rho^2 S^4 \qquad (3)$$

where P_{fo} is the value given in Fig. 2 and

$$S = (\text{Plasma circumference}/2\pi a). \qquad (4)$$

The quantity, a, is the plasma half-width at the midplane (i.e., the plasma radius for a circular device). The neutron wall loading for a circular plasma is given by $0.40 P_f a_p^2/a_w$, where a_p is the plasma radius and a_w is the wall radius. Figure 3 shows the wall loading for circular and rectangular cross-section plasmas, as a function of the maximum magnetic field, for an illustrative set of plasma parameters.

2.2 Determination of the Minimum Test Reactor Size

The test reactor parameters were chosen to minimize power requirements and capital investment, consistent with the following criteria:

(a) Time-averaged neutron wall loading approximately 1 MW/m^2.

(b) Useful wall testing area of at least 10 m^2.

(c) Ease of access for replacement of blanket modules.

(d) Confinement of 150-200 keV beams, and attainment of the required bulk-plasma $n_e \tau_E$.

(e) Containment of fusion alpha particles, in order to minimize alpha-wall interactions.

The minimum major radius of the plasma is determined by the minimum core size, the thickness of the TF coil system, and the thickness of the inner shielding. Figure 4 shows a schematic layout of the machine. The dimensions shown were determined according to the following considerations.

The large time-averaged wall loading demands the use of superconducting coils. A reactor constructed in the next decade would probably have to utilize TiNb as the superconductor. We have chosen this material for the three sets of tokamak coils: toroidal field (TF), ohmic heating (OH), and equilibrium field (EF) coils. Since P_f increases extremely rapidly with B_t (cf. Eq. 3), it is necessary to operate at the maximum possible field. We have chosen a maximum field of 80 kG at the coil with TiNb. Methods to achieve higher fields are discussed in Section 6. The cryogenically stabilized TF coil set is described in Section 4 and in further detail elsewhere [10]. The thickness of each coil and its supporting structure is 40 cm.

Also discussed in the next section is the shield on the inside of the torus. It is designed such that the structural material can withstand radiation damage for the life of such a machine (~8-10 years). The shield thickness is adequate to prevent significant heating rates or radioactivity in the superconducting coils caused by neutrons originating from the plasma. The total shield thickness of 80 cm includes a 10 cm graphite layer that moderates the neutron energy thereby reducing radiation damage to the first structural wall.

The design uses a air-core transformer. The diameter of the core is determined by the maximum flux-swing required to start up the plasma current (~2 MA) and to maintain this current for a period up to 50 s, subject to the limitation of 70 kG for the maximum field in the core. A suitable core diameter is 140 cm.

The above considerations result in the location of the inner wall at 2.3 m. We note that the wall loading increases with plasma minor radius so that we first determine the radius at which criterion (a) is satisfied. The plasma size found in this way must be capable of carrying sufficient current, at $q \geq 2.5$, such that criteria (d) and (e) are satisfied. It is evident from Fig. 3, that for relatively small plasmas and with the axial fields available using TiNb, somewhat elongated cross sections are essential to achieve large wall loadings. The minimum plasma radius that provides a neutron wall loading of 1 MW/m^2 is a = 55 cm, for a plasma elongation of 2:1. The plasma current at q = 2.5 is then 2.4 MA, which is adequate for our confinement requirements at T_e = 5.0 keV (see Section 2.3). (Actually q = 3.0 operation, giving I_p = 2.0 MA, is probably adequate for confinement but leads to half the neutron flux.)

The plasma cross section is chosen in the shape of a flattened "D" (S=1.78), because this shape has gross stability to vertical displacements as well as flutes [11]. Furthermore, the inside-D cross section lends itself well to the implementation of a double-null poloidal divertor [12,13] which is deemed necessary for the removal of D and T ions, impurities, and alphas emerging from the discharge, thereby relieving the heat load on the wall. A scrape-off thickness of the order of 20 cm is required for adequate divertor performance.

The size of the vacuum vessel is completely determined by the above considerations. The total wall area is 149 m^2.

2.3 Plasma Engineering

The plasma parameters for the TCT test-reactor reference design are given in Table I. The choice of 5 keV for the spatially averaged plasma temperature is determined by the following considerations: (1) Q should be near unity, in order to minimize the investment in beam injectors, as well as the power demands; (2) Attaining maximum P_f at lower T_e requires an increase in n_e to values which make beam penetration difficult; (3) The required plasma $n_e \tau_E$ of 8×10^{12} cm^{-3} is well below the limitation set by trapped-ion instability diffusion [14]. The poloidal beta is chosen somewhat smaller than the MHD limiting value, and the value used here will actually be increased by about 10% due to the pressure of fusion alphas. While tokamak plasmas to date have operated in quasi-steady-state only at $\beta_p \lesssim 1 \ll R/a$, experiments have been performed [15,16] in which β_p was increased well above unity by an abrupt decrease in the plasma current, with apparently no adverse effect on the plasma equilibrium.

Profiles of n_e, T_e, and current density, J, are shown in Fig. 5. These profiles of n_e and T_e are expected with the use of an "unload" divertor [13]. J(r) increases slightly faster than $T_e^{3/2}$. For a value of q equal to 2.5 at the limiter, the q on axis is 1.1.

At T_e = 5 keV, there is little variation in Q for W_o in the range 150-225 keV. The value of W_o should then be chosen to maximize the efficiency of producing the beam while assuring adequate beam penetration. With the development of suitable direct conversion techniques [17], or the use of negative ion beams, an efficiency of 65% (busbar to beam) can be expected at 200 keV. The parameters of the beam injectors for the test reactor are given in Table 2. A total power of 200 MW is specified (in the D° component), rather than the 177 MW actually required (Table I), because a small fraction of the injected neutrals is not trapped by the plasma, and the extra power also provides us with a small reserve. The fraction of the wall area taken up by the beam apertures is less than 1%. All vacuum pumping can be carried out through the beam lines, and through the divertor channels.

The trapping profiles of tangentially injected 200 keV neutrals are shown in Figure 6 for a plasma with $Z_{eff} = 1$. Penetration is acceptable, but would be unsatisfactory for 150 keV beams. The ionization cross section of high energy beams increases nearly proportionally to Z_{eff}, so that if $Z_{eff} > 1$, oblique injection must be used in order to maintain good penetration. Figure 6 also shows the trapping profile for perpendicularly injected 200 keV beams in the case of $Z_{eff} = 3$. Apparently, if $Z_{eff} \gtrsim 4$, W_o must be raised above 200 keV, or n_e must be reduced. For $Z_{eff} = 1$, the fraction of injected neutrals trapped in the plasma is 99% and 97% for parallel and anti-parallel injection, respectively, while for Z_{eff}=3 and perpendicular injection, 93% of the neutrals are trapped.

The confinement of alpha-particles in tokamak plasmas has been discussed in Ref. 18. In the test reactor, 92% of the alphas are confined at I_p = 2.4 MA (q = 2.5), and 87% at I_p = 2.0 MA (q = 3.0). This good confinement arises for a number of reasons: (1) The alpha source function is peaked; (2) The aspect ratio of 5.5 results in relatively small banana widths; (3) The scrapeoff layer of 20 cm effectively increases the plasma thickness; (4) The TF ripple at the plasma surface is only 1/4%.

The reference plasma design outlined in Table I specifies a plasma radius at the midplane of 0.55 m with a shape factor S = 1.78 and β_p = 3.5. Initial calculations of MHD equilibrium and stability have been made using the MHD program of Grimm, et al [19]. The usual magnetic-flux equation

$$R \frac{\partial}{\partial R}\left(\frac{1}{R}\frac{\partial \psi}{\partial R}\right) + \frac{\partial^2 \psi}{\partial z^2} = -RJ_\phi = -R^2 \frac{dp}{d\psi} - R^2 B_o^2 g \frac{dg}{d\psi} \qquad (5)$$

is solved in an axisymmetric system to determine the plasma equilibrium for reasonable prescriptions of the pressure profile, $p(\psi)$, and the toroidal field profile, $B_o g(\psi)$. B_o is the vacuum toroidal field on axis, R, ϕ, and z are the usual axisymmetric coordinates with ϕ ignorable, and ψ is the poloidal flux function.

The result of these initial calculations is that an equilibrium configuration can be found with parameters acceptably close to those given in Table I. (The latter parameters were determined on the basis of overall system requirements.) The cross section of a 2.4-MA plasma is shown in Fig. 7 together with the positions of the vertical field coils, and the currents carried by each coil. The height-to-width ratio is 2.75, the shape factor is S=2 and β_p = 3.5. The major radius is 3.0 m, the plasma radius at the mid-plane is 0.46 m, and the magnetic axis is located at 3.1 m. The magnetic field at the shifted magnetic axis is 40 kG. The plasma current profile, averaged over magnetic surfaces, is relatively flat; the safety factor, q, varies from 2.6 on the outside to about 1.5 near the magnetic axis. Tests of the stability criteria for local interchange modes [20] indicate that the plasma is stable. (The program does not now test for stability against toroidal kink modes.) The main conclusions to be drawn are that MHD equilibrium can be found for a plasma with parameters reasonably close to those listed in Table I, and that stability tests to date are favorable. A more complete discussion of these calculations is given by Yang and Conn [21].

Finally, we must consider the duty factor for such a reactor. The operating cycle of a TCT consists of (1) gas filling, (2) discharge current rise and startup of beam injectors, (3) operation at full injector power, (4) shutoff of injectors and reduction of current, and (5) vacuum system purge. The duty factor is the ratio of period (3) to the total cycle period and is determined by the maximum duration of the ohmic discharge, impurity buildup in the plasma, and refueling techniques.

In order to maintain the plasma current, the primary current of the air-core transformer must be increased linearly with time. For the dimensions of Fig. 4, the discharge period can be as long as 50 s. At least 10 s is required to reduce I_p, to purge the vacuum system and refill, and to bring I_p up to the maximum operating value of 2.4 MA. Thus, the duty factor could be as large as 0.83. High current neutral injectors are presently capable of 0.3 s pulses, and there appear to be no insuperable obstacles to steady-state injection. We assume that divertor technology, as developed in PDX [13] and other devices, will be effective in maintaining $Z_{eff} \lesssim 3$, in the case of heavy ions, or $Z_{eff} \lesssim 1.5$ in the case of carbon [22], for periods up to 50 s.

The lifetime of tritons in the plasma, τ_p, is expected to be long compared to τ_E, which includes all transport and radiation losses. The lifetime of thermalized deuterons should be approximately $\tau_p - \tau_s$, since there is a gradual diffusion outward of fast deuterons during their slowing down. (That is, thermalized deuterons have a smaller diffusion scale length than do the tritons.) At T_e = 5.0 keV, the proportion of tritons among the bulk-plasma ions is $f_T = [1 + 0.15\ (\tau_p/\tau_s - 1)]^{-1}$. For the plasma conditions of Table I, τ_p should be of order 300 ms [17], for which f_T = 0.82. Taking into account bulk-plasma DT reactions, the neutron output will be reduced by about 15%.

The tritium composition must be maintained by injection of pellets [23]. Pellet injection into tokamak plasmas is a technology yet to be developed, but it appears to be feasible for a plasma of relatively small density-radius product, such as the present design. Penetration to the center of the plasma requires 1-mm diameter pellets, accelerated to 10 MV [20]. Maintaining f_T = 0.82 requires an injection rate of approximately 60 pellets per second. While it is possible to raise f_T by increasing the rate of pellet injection beyond 60 s^{-1}, T_e will be reduced if the beam input power is constant, so that the neutron output might not be increased.

The principal role of the poloidal divertor in the test reactor is to minimize the number of energetic particles striking the wall, and thereby reduce the impurity influx into the discharge. The plasma capture efficiency must be close to unity, so that the divertor entrance width should be at least 30 cm. Backflow of neutrals into the torus must be prevented (i.e., recycling coefficient $R_n \approx 0$), in order to minimize charge-exchange loss of fast ions, as well as charge-exchange neutral sputtering. The required cryogenic pumping surfaces can be readily accommodated inside the large TF coils. With this unload divertor, the plasma flow in the scrape-off region proceeds nearly at the sound speed [13], the density here is relatively low ($\sim 2 \times 10^{13}$ cm^{-3}), and the plasma temperature is high (~2 keV), as shown in Fig. 5. These characteristics are favorable for a beam-injected reactor.

3. BLANKET AND SHIELD ANALYSIS

An engineering test reactor should be designed as flexibly as possible with ready access to segments which must be changed often, particularly test sections. In a torus, this can be especially complicated if the inner portion nearest the main centerline must be removed. We describe here an approach to avoid this difficulty.

It is a well-known conclusion of recent fusion reactor design studies [1] that the structural materials will have relatively short lifetimes in the radiation environment of a D-T fueled fusion reactor. For example, it has been concluded that a vacuum wall made from 316 stainless steel can be expected to have an average life on the order of two years when subjected directly to a 14 MeV neutron wall loading of 1 MW/m^2. The mechanism limiting wall life depends on several factors, including the operating temperature, and can be related to the high atom displacement rates and high gas production rates (particularly He) expected in such an environment.

For the test reactor described here, we would like to protect the structural wall on the inner portion of the torus. Blanket and shield zones on the outer portion can be removed periodically since this is where access is most readily available. Indeed, this zone can be constructed in a modular fashion as discussed, for example, by the Culham group [25,26] and such modules would themselves serve as test sections. In a recent paper [8], several new concepts for fusion reactor blanket design were presented based on the idea of shifting, or tailoring, the neutron spectrum incident on the first structural wall. The spectral shifter is a non-structural element which can be made of graphite, silicon carbide, or three-dimensionally woven carbon fiber [27]. It would be placed between the neutron source and the first structural wall and serves to soften the neutron spectrum incident on the structural components. This in turn leads to lower gas production and atom displacement rates than in more standard fusion blanket designs and results in longer anticipated lifetimes for the structural materials. It can also significantly reduce radioactivity and afterheat levels. This general class of blanket design concepts was referred to as Internal Spectrum Shapers and Energy Converters, or ISSEC, concepts.

The purpose behind the ISSEC design [8] is to allow the structural components behind the nonstructural spectrum shifting zone to be able to last the plant life. However, for an engineering test reactor, we want the radiation damage on test areas to take place in as short a time as possible. Therefore, in the design discussed here, we propose to use the ISSEC concept only on the inner portion of the torus and, perhaps selectively, on the outer portion. The basic idea is illustrated in Fig. 8. A similar notion has also recently been discussed by Powell and Lazereth [28] and by Sze and Conn [29].

Neutrons from the plasma must pass through the graphite zone before reaching the first structural wall on the inner portion of the torus. In the process, many are slowed down (primarily by the $(n,n')3\alpha$ reaction in carbon), so that the high energy flux above 3 MeV is greatly reduced. This in turn leads to a reduction in displacement damage and gas production in the inner structure. Of course, the unprotected structure on the outer portion is damaged more rapidly, as is desired in a test reactor. The heat deposited in the ISSEC zone (in this case graphite) is conducted to the front and back surfaces and radiated to the cooler outer and inner walls, respectively.

For illustrative purposes, we have examined in detail the nuclear performance of a blanket-shield outlined in Fig. 4. The blanket-shield zones must serve to remove heat and to attenuate neutrons. In particular, for superconducting toroidal field coils, the blanket-shield zones serve to limit the heat deposition in the coils and, as importantly, to limit radiation damage to the copper conductor stabilizing material [30]. The inner shield shown as zone 4 is composed of 70% stainless steel and 30% boron carbide, which has previously been shown to be a very effective design [31]. The coolant would probably be helium. An alternate and equally reasonable design would be to use stainless steel cooled with borated water flowing at high velocities and low pressures to remove the heat [32]. This can keep the blanket-shield temperatures relatively low and reduce thermal stress problems. Either design is feasible and we consider the former design for illustration. Zone 6 on the inside portion of the torus between the plasma and the inner shield is the nonstructural, neutron spectrum shifting zone. Its role is to

protect the structural material in the inner shield. On the outer portion of the torus, there is a 316 stainless steel wall followed by a zone of structural material and coolant. If it is possible to continuously buy tritium for reactor operation, then this outer zone would be designed similarly to the inner shield and would probably be cooled with borated water. However, if it is necessary to produce roughly the amount of tritium consumed, one can achieve this by using liquid lithium at relatively low pressure as the coolant and breeding material on the outer half of the torus. Designs for achieving low pressure lithium cooling in ISSEC blanket designs are discussed by Sze and Conn [29]. Since this is the more interesting case, we examine it and leave the case of cooling with borated water as the more likely and more straightforward alternative.

The nuclear performance of this blanket and shield design has been studied by solving the discrete ordinates [33] form of the transport equation for the neutron and gamma fluxes using the ANISN program [34] in the S_4-P_3 approximation and slab geometry. As noted by Dudziak [35], S_4-P_3 calculations are adequate to predict integral parameters, such as tritium breeding and gas production rates, to within approximately 2% of a high-order calculation like S_{16}-P_5. An albedo of 0.3 in all groups has been used at the back of the outside blanket and no shield has been included there. The neutron and gamma multigroup cross sections were processed using the programs SUPERTOG [36] and MUG [37] from nuclear data compiled in ENDF/B3 [38] with the program, LAPHANGAS [39], except for ^{6}Li, ^{7}Li and C for which the photon cross sections are from reference [40]. All calculations were performed using 46 neutron groups and 43 gamma groups in a group structure discussed in detail previously [1]. The use of slab geometry allows us to simulate different blanket-shield designs on the inner and outer parts of the torus without having to resort to expensive, two-dimensional cylindrical calculation.

The results are listed in Table III. The breeding ratio is 0.8 which means that only 20% of the tritium consumption will have to be provided from off-site. The total energy generated per fusion neutron is 17 MeV. This energy will be removed but not converted to electricity, since the additional costs associated with a power cycle are not justified in light of the purpose of this type of machine.

The principal radiation damage characteristics of the first inner wall behind the graphite spectral shaping zone (zone (5) in Fig. 4) and the vacuum wall on the outer portion of the torus (zone (7) in Fig. 4) are also given in Table III. The displacements per atom (dpa) rate in zone (5) is 5.18 dpa/yr for a wall loading of 1 MW/m^2. By contrast, the first wall on the outer half of the torus experiences 15.64 dpa/yr. Thus, the inner structural wall (zone (5)) will have at least three times the wall life compared with zone (7) when only a 10 cm graphite zone is used. Thicker zones are possible from a heat transfer viewpoint but 10 cm appears adequate for the purpose here. The helium and hydrogen production rates are also given for these two zones. The decrease for zone (5) is even larger than for the dpa rate because the cross sections for hydrogen and helium production have a threshold behavior such that neutrons below about 3 MeV do not significantly contribute to the gas production. This is not the case for displacement damage.

The energy attenuation of the inner blanket-shield design is 8.31×10^{-6} and the energy attenuation of the blanket and shield on the outer portion of the torus will be at least an order of magnitude greater. Therefore, with a 1 MW/m^2 wall loading of 14 MeV neutrons, the heat deposition in the superconducting coils is approximately 625 W. Assuming it takes 500 W at 300°K to remove 1 W at 4.2°K [4], the refrigeration power required for the TF magnets is approximately 0.3 MW.

Perhaps more important is the dpa rate in the copper stabilizer of the magnet. This rate varies from 4×10^{-4} dpa/yr at the magnet winding closest to the plasma (point A in Fig. 9) to $6x2 \times 10^{-5}$ at point B. The effect will be to increase the resistivity of PFHC copper by approximately a factor of 4 in one year. While this problem can be corrected by periodic annealing, it can probably be avoided by a redesign of the inner shield to include a non-uniform distribution of boron carbide and stainless steel [42]. This redesign can reduce the dpa levels in the Cu to where annealing once every one to two years will be satisfactory.

The next major question relates to the heat deposition and operating temperature of the inner graphite zone (zone 6 in Fig. 4). The nuclear heat deposition from neutrons and gammas serves as input to the heat transfer calculations. Heat is assumed to be conducted to the front and back surfaces and radiated to the colder stainless steel walls. The temperature distribution in the graphite spectrum shaper is insensitive to the actual stainless steel temperatures as long as these are low. Since the graphite will be at least 1000°C while the stainless steel will be 500°C or less (and perhaps only 100-200°C), this condition is satisfied. The thermal conductivity has been taken as that of nuclear grade graphite, namely 0.36 W/cm-°C. The temperature profile in the graphite is shown in Fig. 10 for a neutron wall loading of 1 MW/m^2 and a surface heat loading of 50 W/cm^2. The maximum temperature is 1650°C which is well below the 2000°C range where the vapor pressure of graphite becomes comparable to the pressure in the plasma chamber (namely 10^{-6} to 10^{-5} torr). This problem has been extensively reviewed elsewhere [22].

An important variation on this result is to consider the effect of the surface heat flux on the maximum temperature. The low $n\tau$-values typical of TCT operation may result in high surface heat loads, depending on whether a divertor is used and on the severity of impurity radiation. In Fig. 11, we show the variation in the maximum graphite temperature as a function of surface heat load. It appears that even under very high surface loadings, such as 100 W/cm^2, the maximum temperature remains within the acceptable range.

From these results, we conclude that the ISSEC concept can extend the life of the shield on the inner portion of the torus. The test modules making up the outer portion of the torus will be subject to higher 14 MeV fluxes and will be damaged more rapidly. These modules can be readily removed and replaced since the outer part of a torus is where space is plentiful. Thus, this blanket-shield concept, when combined with the toroidal field coil design discussed next, brings considerable flexibility to toroidal systems.

4. SUPERCONDUCTING TF COILS

Superconducting toroidal field magnets are practically mandatory for the machine described here in order to minimize power consumption and insure a relatively long pulse with a large duty factor. The detailed superconducting magnet design will be presented elsewhere [10], but for completeness we describe and summarize the main features here. (We have investigated the use of a water cooled copper magnet set; although steady-state operation with an axial field of 30 kG is possible, the power consumption is at least 180 MW.)

The toroidal field coils have been designed with the philosophy of complete cryogenic stability, in order to insure maximum reliability, and with as little extrapolation of present technology as possible. This dictates the choice of TiNb superconductor filaments embedded in a copper matrix. A copper backing strip is included to guarantee complete cryogenic stability, and liquid helium pool boiling at 4.2°K is used for cooling the conductor. The design maximum field at the conductor is 80 kG at 4.2°K. Pumping the helium bath to lower temperatures can allow the coils to operate at even higher fields [41].

The "embedded disc" type conductor design developed by Boom, Young, et.al. [41], is used. The structural material for the coil is 316 stainless steel. The shape of the magnets is a modified or extended "D" shape as shown in Fig. 9. This shape, as developed in the UWMAK-II conceptual reactor design [9], provides extra space for removing blanket-shield modules on the outer portion of the torus while maintaining a height no more than is required for the internal system components, including the vertical field coils.

The major characteristics of the toroidal field coils are listed in Table IV. The average current density is about 2800 A/cm^2. The total number of coils is 18, and an analysis of the field structure shows that the maximum field ripple at the outer surface of the plasma is less than 0.22%.

Lue and Conn [10] have carried out an estimate of the total capital cost of this toroidal field coil set and arrive at amounts between 5 and 13 million dollars depending on the price of the superconductor. This can be compared with cost estimates for similar coils recently compiled by Lubell [43]. The total energy stored in the toroidal field of the coil set described in Table IV is approximately 2600 MJ and, with this as input, the cost estimate based on Lubell's compilation turns out to be between 6 and 13 million dollars, in good agreement with the values of Ref. [10].

5. POWER REQUIREMENTS AND COST ESTIMATES

The power ratings of the various electrical systems of the test reactor are given in Table V. As noted before, the OH and EF coils are constructed of TiNb, since the power dissipation in copper coils would be prohibitively large. The parameters of the OH and EF electrical systems are given in Table VI. Since the peak power requirement of the OH circuit (42 MW) occurs during discharge current startup (that is, before beam injector turn-on), the OH coils can be supplied directly from the power line without affecting the maximum power to be drawn from the line. Otherwise, a 28 MJ energy storage system is required to supply the OH coils during startup.

We have considered variations of B_t and b/a, keeping q and β_θ fixed, to determine the effect on the 14-MeV neutron wall loading. The results are summarized in Fig. 12. If the height-to-width ratio is increased to 3 and the shape factor S is taken as 2.35, with B_{tmax} held at 80 kG, the plasma current is increased to 4.5 MA, the power density becomes 13 W/cm^3, the wall area is 195 m^2 and the neutron wall loading is 3.4 MW/m^2.

If the height-to-width ratio remains 2 but the maximum field is increased to 90 kG by pumping on the helium to ~3°K, the plasma current increases to 2.7 MA, the fusion power density increases to 6.9 W/cm^3, and the neutron wall loading becomes 1.54 MW/m^2, a 50% gain in wall loading compared with the base case. This case is likely to be the most straightforward of the magnet alternatives to achieve.

For the Nb_3Sn cases, the maximum field is taken as 150 kG. For a 2:1 noncircular machine with the dimensions of the base case, the plasma current is 4.47 MA, the fusion power density is 53 W/cm^3 and the neutron wall loading is 11 MW/m^2. This value is probably too high even for a test reactor, and the correspondingly high plasma density would require neutral beam energies much greater than 200 keV.

With 150 kG maximum field, it is interesting to examine a circular machine of comparable size. For illustration, consider a device with a plasma current of 2.5 MA at q = 2.5 and a radius to the innermost coil winding of 1.45 m, as chosen previously. The resulting plasma radius is 79 cm, the major radius is 3.3 m, and the wall area with a 20 cm scrape-off zone is 130 m^2. The axial magnetic field becomes 66.2 kG, the fusion power density is 10.5 W/cm^3 and the 14 MeV neutron wall loading is 3.3 MW/m^2.

We see from these calculations of design alternatives that there can be many tokamak plasmas in approximately the same overall size range which generate neutron wall loadings of 1 MW/m^2 or greater. Such devices could perform the function of an engineering test reactor.

ACKNOWLEDGMENTS

The authors thank M. Gohar, W. Lue, and D. K. Sze for informative discussions and help with some of the calculations. This research was supported by the United States Energy Research and Development Administration and the Wisconsin Electric Utility Research Foundation.

The EF coils, on the other hand, demand substantial power during both current startup and the period when the plasma is being heated and β_p is being raised to its final value. The total EF energy during the current startup and plasma heating phases can be supplied from a capacitor bank. Once plasma conditions reach equilibrium, further EF power is supplied directly from the mains, while the capacitor storage is charged for the next cycle.

The current risetime has been chosen to be 1.0 s in order to minimize eddy current dissipation in the TF coils and to minimize the cost of OH electrical equipment, such as rectifiers and switches. The injection current will be brought up to full value over a one second period also, in order to minimize EF power and associated electrical equipment.

The power specified for refrigeration is adequate even if the TF coils are to be maintained at 1.8°K (in order to increase B_t). Miscellaneous plant equipment includes circulation pumps for the blankets, vacuum pumps, power supplies for electronic equipment, and ventilation systems.

The estimated costs of the major systems of the test reactor are given in Table VII. The cost of the neutral beam injectors is estimated as \$0.40/watt, where the power refers to the D° component of the neutral beam. This figure includes the investment in direct conversion, if any, that is necessary to give an efficiency of production (busbar to beam) of 65%, as well as the rather small outlay for rectifiers. (The beam injectors will be supplied directly from the mainline while the EF electrical equipment includes the 20 MJ capacitor bank.) The cost of the TF coil is that estimated in section 4.

With an operating duty factor of 80%, and a particle turnover time of 300 ms, the tritium throughput is 180 g/hr. A plant inventory of about 1 kg of tritium (10 MCi) is therefore required. If the duty factor averaged over the year is 50% (including down time for module replacement), the annual consumption of tritium is 5.0 kg. This amount may be sufficiently small that tritium need not be bred in the test reactor blanket, thereby reducing blanket and processing costs. However, as discussed in section 3, the option exists of designing Li-bearing blankets that can give breeding ratios of about 0.8 (and higher if Be is used). Thus, the tritium required from off-site could be reduced by at least 80%.

6. ALTERNATIVE PLASMA AND MAGNETIC FIELD ASSUMPTIONS

For the base case design discussed in sections 2, 3, and 4, the plasma cross-section was taken as noncircular with a height-to-width ratio of 2 and the maximum toroidal field strength was limited to 80 kG. However, both B_t and b/a might be increased. There are two possible ways of increasing B_t. First, at least 90 kG can be obtained even with TiNb superconductor by pumping on the He coolant and operating as low as 1.8°K [43]. Second, Nb_3Sn with its much higher critical field could in principle be used as the superconductor. This material is much more brittle than TiNb (which is the reason we did not choose it for base case calculations) but nevertheless provides an interesting alternative. It has been considered recently in a fusion reactor conceptual design study [2].

REFERENCES

1. B. BADGER, et al, "UWMAK-I, A Wisconsin Toroidal Fusion Reactor Design," UWFDM-68, Nuclear Eng. Dept., Univ. of Wisconsin (Nov. 1973), Vol. I.

2. R. G. MILLS, ed., "A Fusion Power Plant," Princeton Plasma Physics Lab. Report MATT-1050 (Aug. 1974).

3. K. SAKO, et al, "Conceptual Design of a Gas-Cooled Tokamak Reactor," in *Fusion Reactor Design Problems*, International Atomic Energy Agency, Vienna (1974), p. 27.

4. T. H. BALZER, et al, "Conceptual Design of a Mirror Reactor for a Fusion Engineering Research Facility (FERF)," Lawrence Livermore Lab. Report UCRL-51617 (Aug. 1974).

5. M. A. ABDOU, et al, "Engineering Design of an FTR and FERF Based on a Toroidal Theta Pinch," *Proceedings of Fifth International Conference on Plasma Physics and Controlled Nuclear Fusion Research*, International Atomic Energy Agency, Tokyo (1974), to be published.

6. J. M. DAWSON, H. P. FURTH, F. H. TENNEY, *Phys. Rev. Lett.*, 26, 1156 (1971). See also H. P. FURTH and D. L. JASSBY, *Phys. Rev. Lett.*, 32, 1176 (1974).

7. D. L. JASSBY, "Optimization of Fusion Power Density in the Two-Energy-Component Tokamak Reactor," Princeton Plasma Physics Lab. Report MATT-1072 (Oct. 1974); to be published in *Nuclear Fusion*. See also D. L. JASSBY, "Beam Driven Tokamak Fusion - Fission Hybrid Reactors," Princeton Plasma Physics Lab. Report MATT-1115 (March, 1975), published in ERDA-4, S. L. BOGART, ed., pp. 221-245 (1975).

8. R. W. CONN, et al, "New Concepts for Fusion Reactor Blanket Design," *Nuclear Technology* 26, 125 (1975).

9. R. W. CONN, et al, "Major Design Features of the Conceptual D-T Tokamak Power Reactor, UWMAK-II," *Proceedings of Fifth International Conference on Plasma Physics and Controlled Nucl. Fusion Research*, IAEA, Tokyo (1974), Paper CN-33/G1-2, to be published.

10. J. W. LUE, R. W. CONN, "Superconducting Toroidal Field Magnets for a Tokamak Engineering Test Reactor," *Proceedings 1975 Cryogenic Engineering Conference*, Kingston, Canada (July, 1975), to be published.

11. M. OKABAYASHI, G. SHEFFIELD, *Nucl. Fusion* 14, 263 (1974).

12. G. A. EMMERT, A. T. MENSE, M. J. DONHOWE, "A Poloidal Divertor for the UWMAK-I Tokamak Reactor," *Proceedings 1st Top. Meet. on the Tech. of Cont. Nucl. Fusion*, USAEF Conf.-740402-P1 (1974), p. 417.

13. D. M. MEADE, et al, "The Effects of Impurities and Magnetic Divertors on High Temperature Tokamaks," *Proc. 5th International Conf. on Plasma Physics and Cont. Nucl. Fus. Research*, IAEA, Tokyo (1974), Paper CN-33/A 15-4, to be published.

14. S. O. DEAN, et al, "Status and Objectives of Tokamak Systems for Fusion Research," USAEC Rep. WASH-1295 (July 1974).

15. S. V. MIRNOV, *JETP Lett.* 12, 64 (1970).

16. J. C. HOSEA, Princeton Plasma Phys. Lab. Report MATT-1128 (April 1975).

17. J. HOVINGH, R. W. MOIR, *Nucl. Fusion* 14, 629 (1974).

18. D. G. MCALEES, "Alpha Particle Energetics and Neutral Beam Heating in Tokamak Plasmas," Oak Ridge National Lab. Report ORNL-TM-4661 (1974).

19. R. C. GRIMM, J. M. GREENE, J. L. JOHNSON, and R. L. DEWAR, *Journal of Computational Physics*, to be published.

20. M. S. CHANCE, et al, *Proceedings of 5th Internationa Conf. on Plasma Physics and Cont. Nuc. Fus. Research*, IAEA, Tokyo (1974), Paper CN-33/A 12-4, to be published.

21. T. YANG and R. W. CONN, to be published.

22. G. L. KULCINSKI, R. W. CONN, G. LANG, *Nucl. Fusion* 15, 327 (1975).

23. S. GRALNICK, *Nucl. Fusion* 13, 703 (1973). See also Ref. 2, Ch. 7.

24. G. L. KULCINSKI, et al, *Nucl. Technology* 22, 20 (1974).

25. J. T. D. MITCHELL, M. W. GEORGE, "A Design Concept for a Fusion Reactor Blanket and Magnet Shield Structure," Culham Lab. Report CLM-R121 (June 1972).

26. J. T. D. MITCHELL, R. HANCOX, "A Lithium Cooled Toroidal Fusion Reactor," Culham Lab. Report CLM-P319 (Aug., 1972).

27. "Carbon Fibers: Their Composites and Applications," *Plastics and Polymers Conf. Suppl. #5*, The Plastics Institute, London (1971).

28. J. POWELL, O. LAZERETH, *Trans. Am. Nucl. Soc.* 19, 17 (1974).

29. D. K. SZE, R. W. CONN, *Trans. Am. Nucl. Soc.* 21, 34 (1975).

30. B. BADGER, et al, op. cit., Chapter 6.

31. M. A. ABDOU, C. W. MAYNARD, "Nuclear Design of the Magnet Shield for Fusion Reactors," *Proceedings 1st Top. Meeting on the Tech. of Cont. Nucl. Fusion*, USAEC Conf.-740402-P1 (1974), p. 685.

32. M. HOFFMAN, R. W. WERNER, "Heat Flux Limitations on First Wall Shields in Early Fusion Machines," *Proceedings 1st Top. Meeting on the Tech, of Cont. Nucl. Fusion*, USAEC Conf-740402-P1 (1974), p. 619.

33. G. I. BELL, S. GLASSTONE, *Nuclear Reactor Theory*, Van Nostrand Reinhold Co., New York (1970), Chapter 5.

34. W. V. ENGLE, JR., "A User's Manual for ANISN," K-1693, Oak Ridge Gaseous Diffusion Plant (March, 1967).

35. D. J. DUDZIAK, "Fusion Reactor Nuclear Analysis-Methods and Applications," *8th Symposium on Fusion Tech.*, EUR 5182e (1974) p. 915.

36. R. Q. WRIGHT, et al., "SUPERTOG: A Program to Generate Fine Group Constants and Pn Scattering Matrices from ENDF/B, Oak Ridge National Lab. Report ORNL-TM-2679 (1969).

37. J. R. KNIGHT, F. R. MYNATT, "MUG: A Program for Generating Multigroup Photon Cross Sections," CTC-17 (Jan., 1970).

38. M. K. DRAKE, Ed., "Data Formats and Procedures for the ENDF Neutron Cross Section Library," BNL-50279, Brookhaven National Lab. (1970). See also O. OZER and D. GARBER, "ENDF/B Summary Documentation", BNL 17541 and ENDF-201 (July, 1973).

39. D. J. DUDZIAK, et al., "LAPHANO: A Po Multigroup Photon Production Matrix and Source Code for ENDF," Los Alamos Sci. Lab. Report LA-4750-MS (1972).

40. GAM-II Cross Section Library. This data is available from the Radiation Shielding Information Center, Oak Ridge National Laboratory.

41. B. BADGER et al., op. cit., Chapter 7.

42. M. GOHAR, private communication.

43. M. S. LUBELL, "Superconducting Toroidal Magnets for Fusion Feasibility Experimental and Power Reactors," Oak Ridge National Lab. Report ORNL-TM-4635 (July, 1974).

TABLE I

Plasma Parameters of a Tokamak Engineering Test Reactor

R_o	3.05 m
a	0.55 m
A	5.55
elongation	2.0
shape factor	1.78 (flattened "D" shape)
horizontal wall radius	0.75 m
wall area	149 m^2
plasma area	2.16 m^2
axial B_t	38.0 kG
I_p	2.4 MA
q	2.5
$\bar{n}_e$	1.2×10^{14} cm^{-3}
$\bar{T}_e = \bar{T}_i$	5.0 keV
$\bar{n}_e \tau_E$	8×10^{12} $cm^{-3}s$
W_o	200 keV
P_{beam}	177 MW
I_{beam}	885 A
β_p	3.5
Q_b (ideal)	1.0
P_f (ideal)	4.3 W/cm^3
$\bar{\Gamma}$	0.85
neutron production	6.4×10^{19} n/s
neutron power	142 MW
neutron wall loading	0.96 MW/m^2
total thermal power	355 MW

TABLE II

Neutral Beam Injection Systems

Injection energy	200 keV
Injection power	200 MW (D°) peak
Injection current	1000 A (equiv) peak
Total beam aperture	1.0 m^2 at 0.1 A/cm^2
Fraction of wall area	0.7%
Overall efficiency	65%
Power consumption	310 MW

TABLE III

Nuclear Characteristics of the Blanket-Shield Design Outlined in Figure 4

Breeding Ratio	0.8
Energy Per Fusion	17.0 MeV
Energy Attenuation by Inner Blanket-Shield per 14 MeV Neutron	8.34×10^{-6}
Displacements per Atom for 1 MW/m^2 Wall Loading	
In zone (5)[a]	5.18 dpa/yr
In zone (7)[b]	15.64 dpa/yr
Helium Production Rate for 1 MW/m^2 Wall Loading	
In zone (5)[a]	58.0 appm/yr
In zone (7)[b]	297.8 appm/yr
Hydrogen Production Rate for 1 MW/m^2 Wall Loading	
In zone (5)[a]	151.0 appm/yr
In zone (7)[b]	615.8 appm/yr

[a] Zone (5) is the stainless steel wall behind the graphite spectrum shaper.

[b] Zone (7) is the stainless steel vacuum wall on the outer part of the torus.

TABLE IV

Principal Characteristics of Superconducting Toroidal Field Magnets

Axial Magnetic Field	38 kG
Maximum Magnetic Field	80 kG
Superconductor	TiNb
Average Current Density in Conductor Discs[a]	2800 A/cm^2
Magnet Cross Section	37cm x 40cm
Disc Cross Section	2cm x 40cm
Discs per magnet	16
Total Cu to TiNb Ratio	6:1
Disc Stainless Steel to Cu Ratio (Cryogenic Stability)	1:2
Number of Coils	18
Radius to Point of Max. Field	1.45 m
Coil Bore at Midplane	5.5 m

[a]The average current density is defined as the ratio of the total current-turns divided by the total area of a winding disc.

TABLE V

Power Consumption

System	Energy Supply	Peak Power
Refrigeration (all coils)	Main Line	5 MW
OH coils (TiNb)	(1) Main Line (current startup)	42 MW
	(2) Main Line	2 MW
Equilibrium field coils (TiNb)	(1) Capacitor bank	28 MW
	(2) Main Line	4 MW
Beam injectors	Main Line	310 MW
Miscellaneous plant equipment	Main Line	20 MW

The maximum power drawn from the main line is 341 MW.

TABLE VI

OH Power System

Plasma current	2.4 MA
Current risetime	1.0 s
Current duration	50 s
Flux swing	26 volt-s
Stored energy for startup (if capacitors used)	28 MJ
Maximum field in core	65 kG
Peak power	42 MW
Peak current	10.5 KA
Peak voltage	4.0 kV

EF Power System

Maximum Vertical Field	5.1 kG
Maximum Rate of Change of Vertical Field	3.0 kG/s
Stored Energy	22 MJ
Peak Power	28 MW
Peak Voltage	0.8 kV
Peak Current	36 kA

TABLE VII

Preliminary Cost Estimates of Major Subsystems of a Tokamak Engineering Test Reactor

Cost Element	Cost (10^6 $)
TF coils and supports	13
OH, EF coils	8
Refrigeration	10
Vacuum vessel and equipment	12
Neutral beam injectors	80
Fuel injection and liquid helium	8
Blanket modules and shielding	55
Tritium inventory	2
Tritium handling system	16
Instrumentation and controls	20
Remote handling	20
Electrical equipment for OH and EF	9
Heat removal and cooling towers	40
Buildings	35
Total of above items[a]	$328 M

[a] One can roughly estimate the total cost of reactor construction and installation by adding 15% to account for engineering services and, if necessary, a percentage to account for contingency.

FIGURE CAPTIONS

Fig. 1. Fusion power gain Q_f vs power density P_f for a D-T plasma with $T_e = T_i$ heated by 200-keV D beams. For each $n_e\tau_e$, the D-T composition of the background plasma is adjusted for maximum Q_f. For each T_e there is a maximum in P_f, while Q_f increases nonotonically with $n_e\tau_E$. The dashed curves are contours cf constant $n_e\tau_E$ ($cm^{-3}sec$). Total plasma pressure - 0.655 J/cm^3. (Taken from Ref.7.)

Fig. 2. Comparison of fusion power density P_f for a TCT plasma with optimal $\bar{\Gamma}$ and a thermal plasma with $\Gamma = 0$. In each case, B_t = 50 kG, A = 3.5, $\beta_p = 3.5$, q = 2.5. Q is the fusion power gain of the TCT plasma. (Taken from Ref. 7.)

Fig. 3. Neutron wall loading for circular and rectangular (b/a=2) TCT reactor plasmas. B_{coil} is the field at the TF inner wall, located at 1.45 m. The vacuum inner wall is at 2.3 m, and the thickness of the scrape-off layer is 20 cm. For the circular case, a=80 cm, A=4.1. For the rectangular case, a=50 cm, A=6.0. Both plasmas have the same cross-sectional area. In each case, β_p=0.5A, q=2.5. The fields at the magnetic axis are indicated.

Fig. 4. The graphite zone (6) protects the inner structural wall zone (5) from excessive radiation damage. The outer blanket contains Li if tritium production is necessary. Otherwise, zone (8) would be cooled with borated water and zones (9) and (10) would be replaced by normal shielding.

Fig. 5. Radial profiles in the plasma midplane. The discharge is confined to $r \leq 55$ cm. The scrape-off region lies between 55 and 75 cm. On-axis parameters are indicated.

Fig. 6. Trapping profiles of 200-keV D neutrals injected into the test reactor plasma. The plasma density profile is shown in Fig. 5.

Fig. 7. Cross-section of the engineering test reactor showing vertical-field coils and their currents.

Fig. 8. Cross-section of the engineering test reactor showing blankets and shielding. The plasma flux surfaces have been calculated with an MHD equilibrium code.

Fig. 9. Shape of the superconducting toroidal field magnet. The blanket and shield extend to approximately 5.25 m, so that modules can be extracted without removing any TF coils.

Fig. 10. Temperature distribution in the graphite ISSEC zone.

Fig. 11. Variation of the maximum temperature in the graphite ISSEC zone as a function of the surface heat load. The 14 MeV neutron wall loading is 1 MW/m^2.

Fig. 12. Wall loading for various values of magnetic field and plasma elongation, b/a.

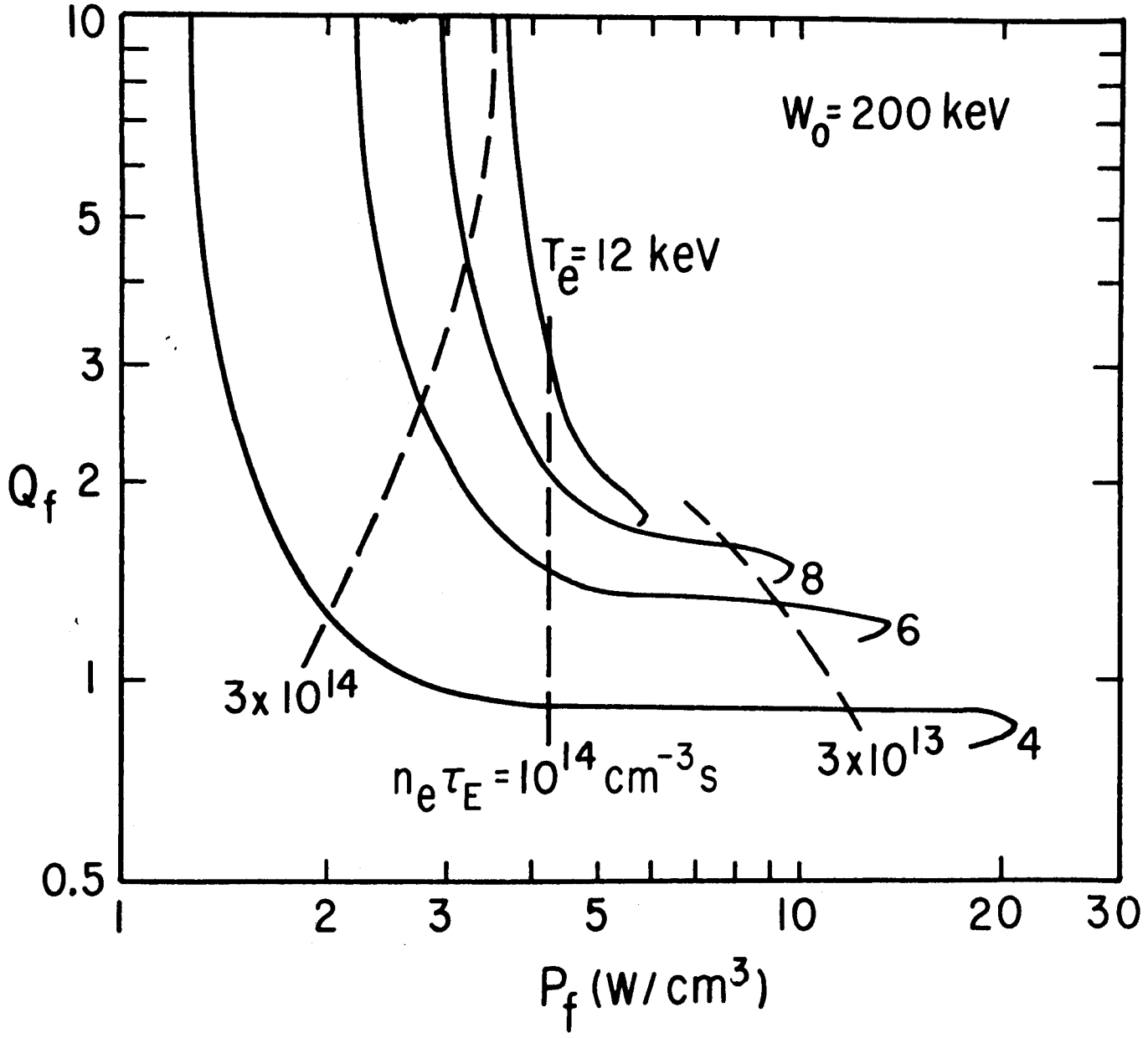
10
5
3
2
1
0.5
Q_f
W_0= 200 kev
T_e= 12 kev
8
6
4
$3x10^{14}$
$3x10^{13}$
$n_e\tau_E = 10^{14}\,cm^{-3}s$
1
2
3
5
10
20
30
$P_f\,(W/cm^3)$

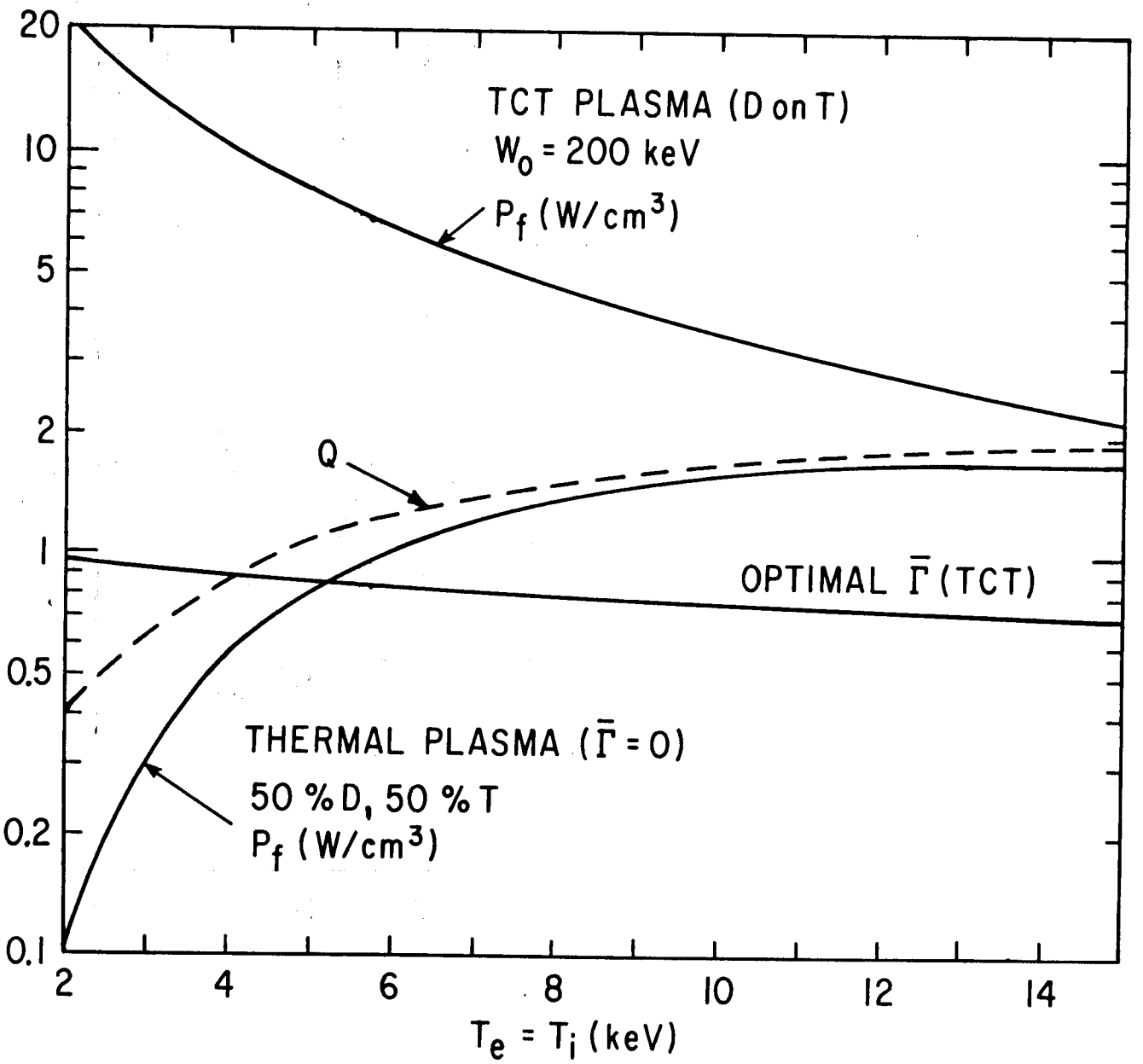
TCT PLASMA (D on T)
W_0 = 200 keV
P_f (W/cm^3)
Q
OPTIMAL $\bar{\Gamma}$ (TCT)
THERMAL PLASMA ($\bar{\Gamma}$ = 0)
50 % D, 50 % T
P_f (W/cm^3)
20
10
5
2
1
0.5
0.2
0.1
2
4
6
8
10
12
14
$T_e = T_i$ (keV)

SCHEMATIC LAYOUT OF BLANKET-SHIELD FOR A TOKAMAK ENGINEERING TEST REACTOR

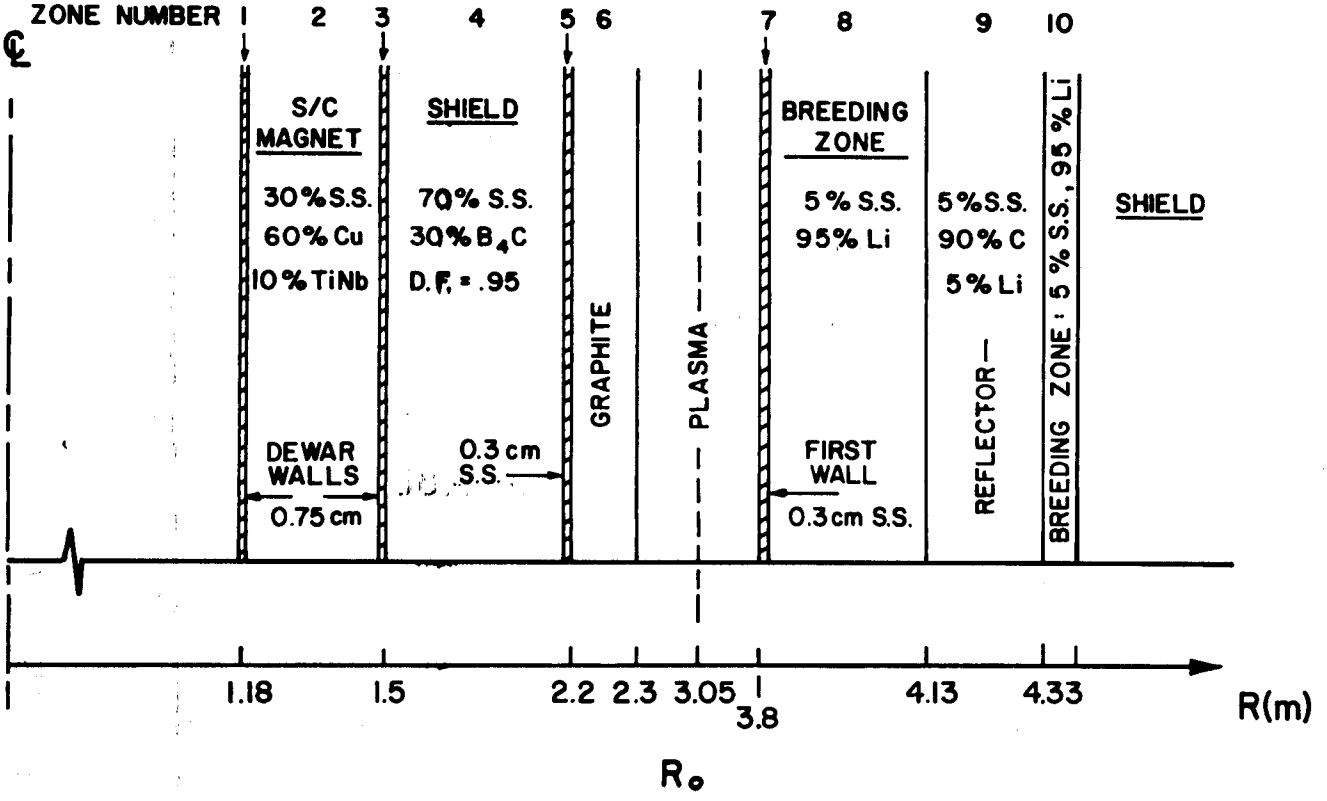

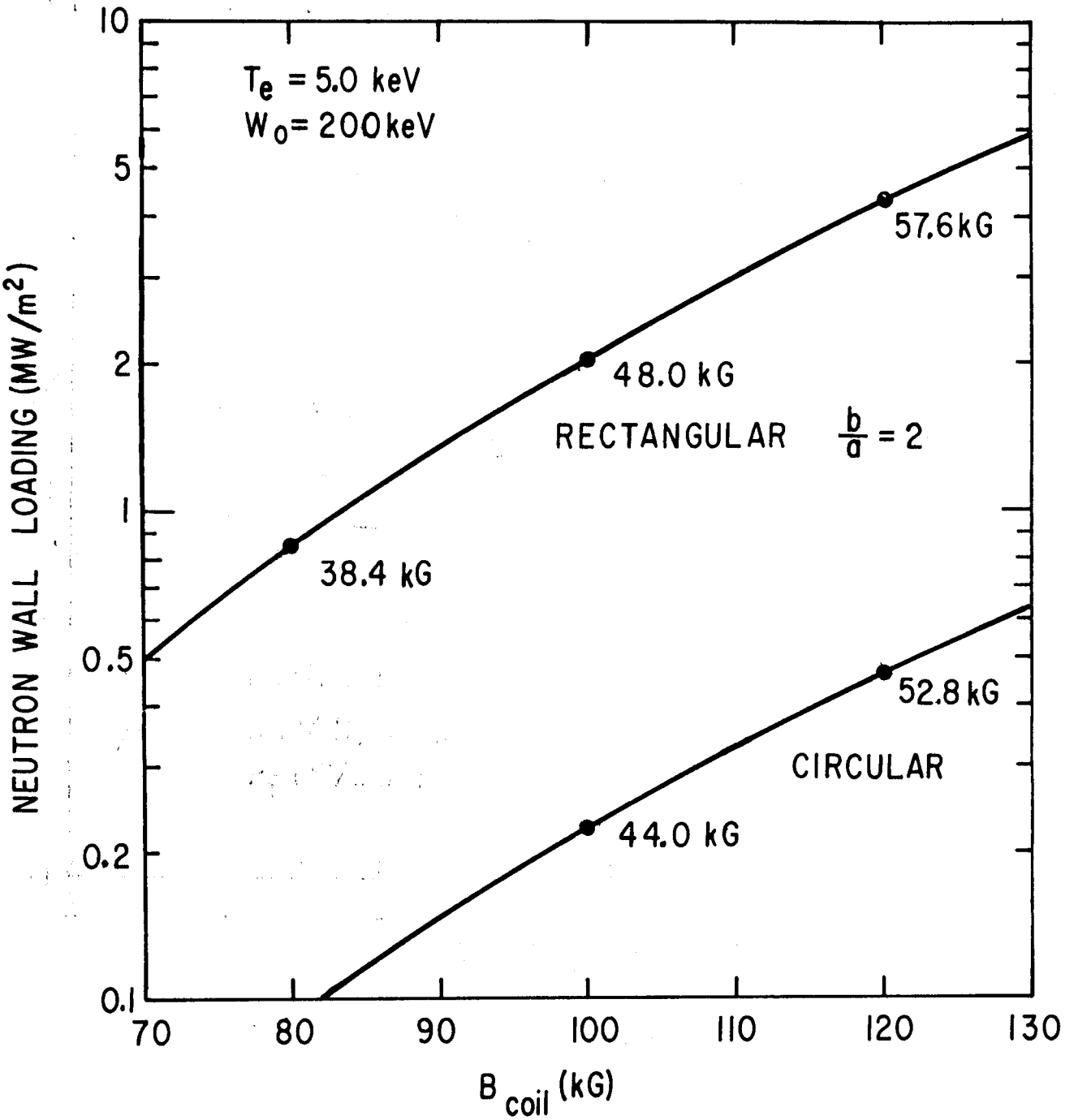
T_e = 5.0 keV
W_0 = 200 keV
57.6 kG
48.0 kG
RECTANGULAR $\frac{b}{a}$ = 2
38.4 kG
52.8 kG
CIRCULAR
44.0 kG
NEUTRON WALL LOADING (MW/m²)
10
5
2
1
0.5
0.2
0.1
70
80
90
100
110
120
130
B_{coil} (kG)

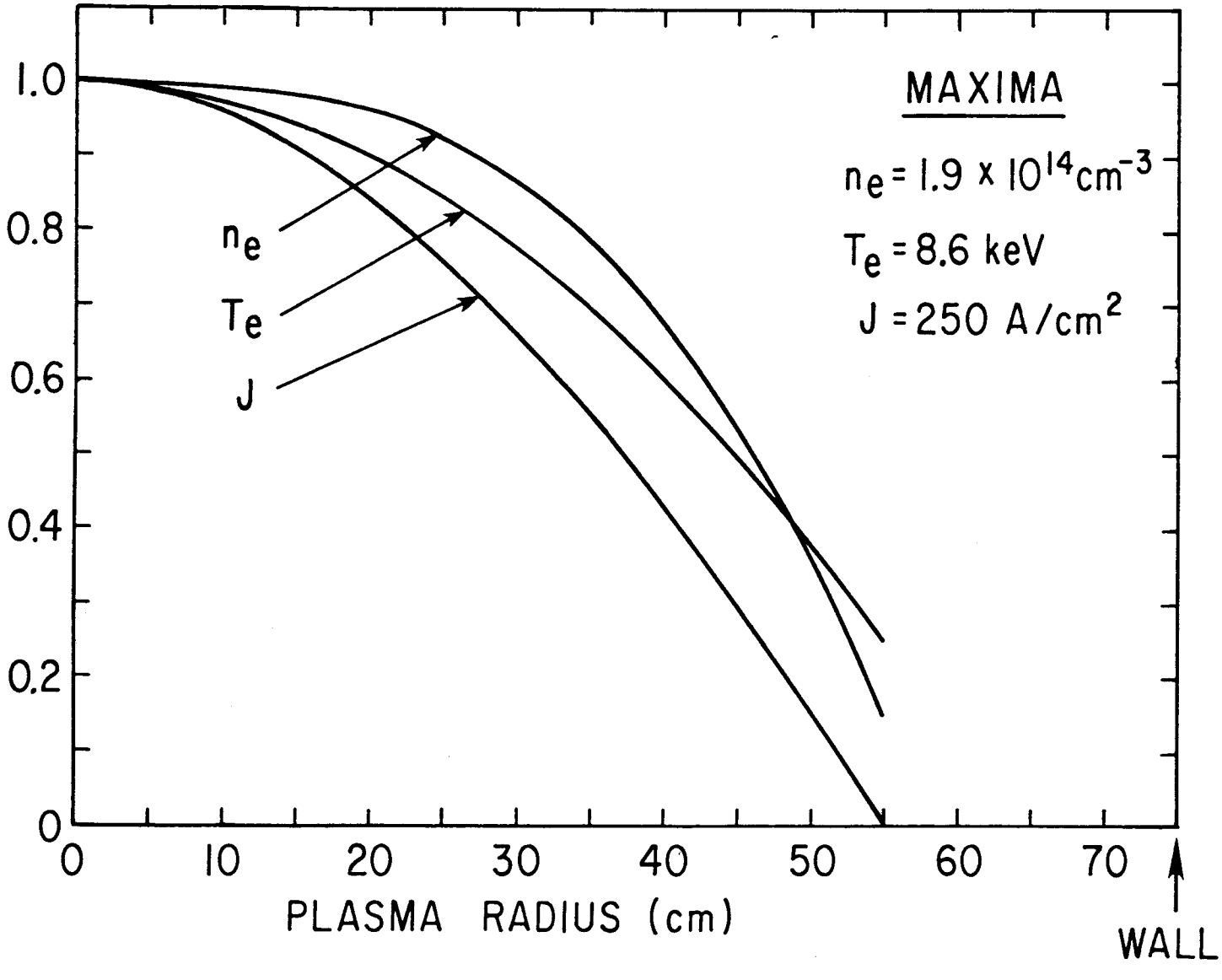
MAXIMA
$n_e = 1.9 \times 10^{14} cm^{-3}$
$T_e = 8.6$ keV
$J = 250$ A/cm^2
n_e
T_e
J
1.0
0.8
0.6
0.4
0.2
0
0
10
20
30
40
50
60
70
PLASMA RADIUS (cm)
WALL

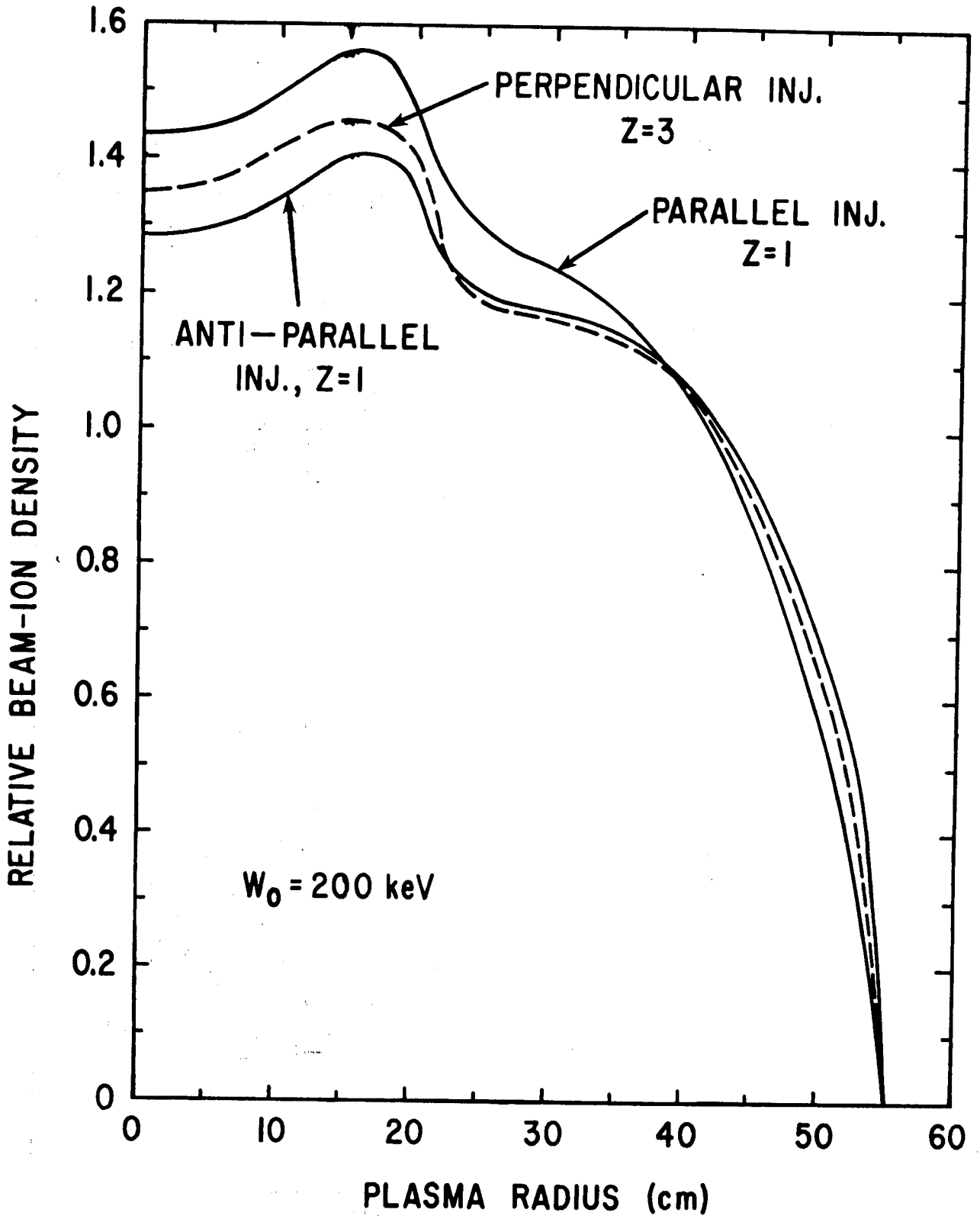
1.6
1.4
1.2
1.0
0.8
0.6
0.4
0.2
0
0
10
20
30
40
50
60
RELATIVE BEAM-ION DENSITY
PLASMA RADIUS (cm)
PERPENDICULAR INJ.
Z=3
PARALLEL INJ.
Z=1
ANTI—PARALLEL
INJ., Z=1
W_0 = 200 keV

"D" SHAPED DISC

OF A TOROIDAL FIELD MAGNET

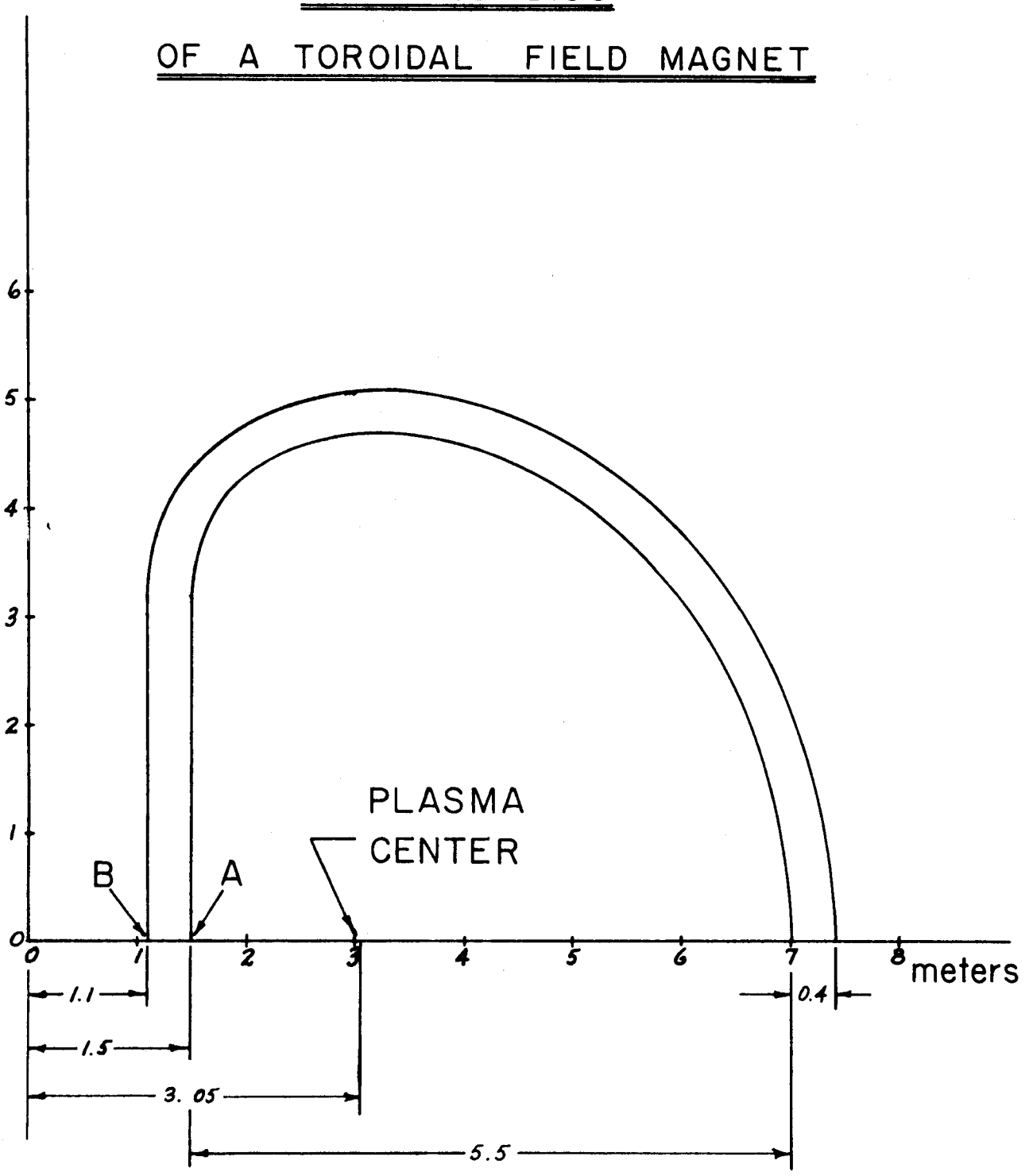

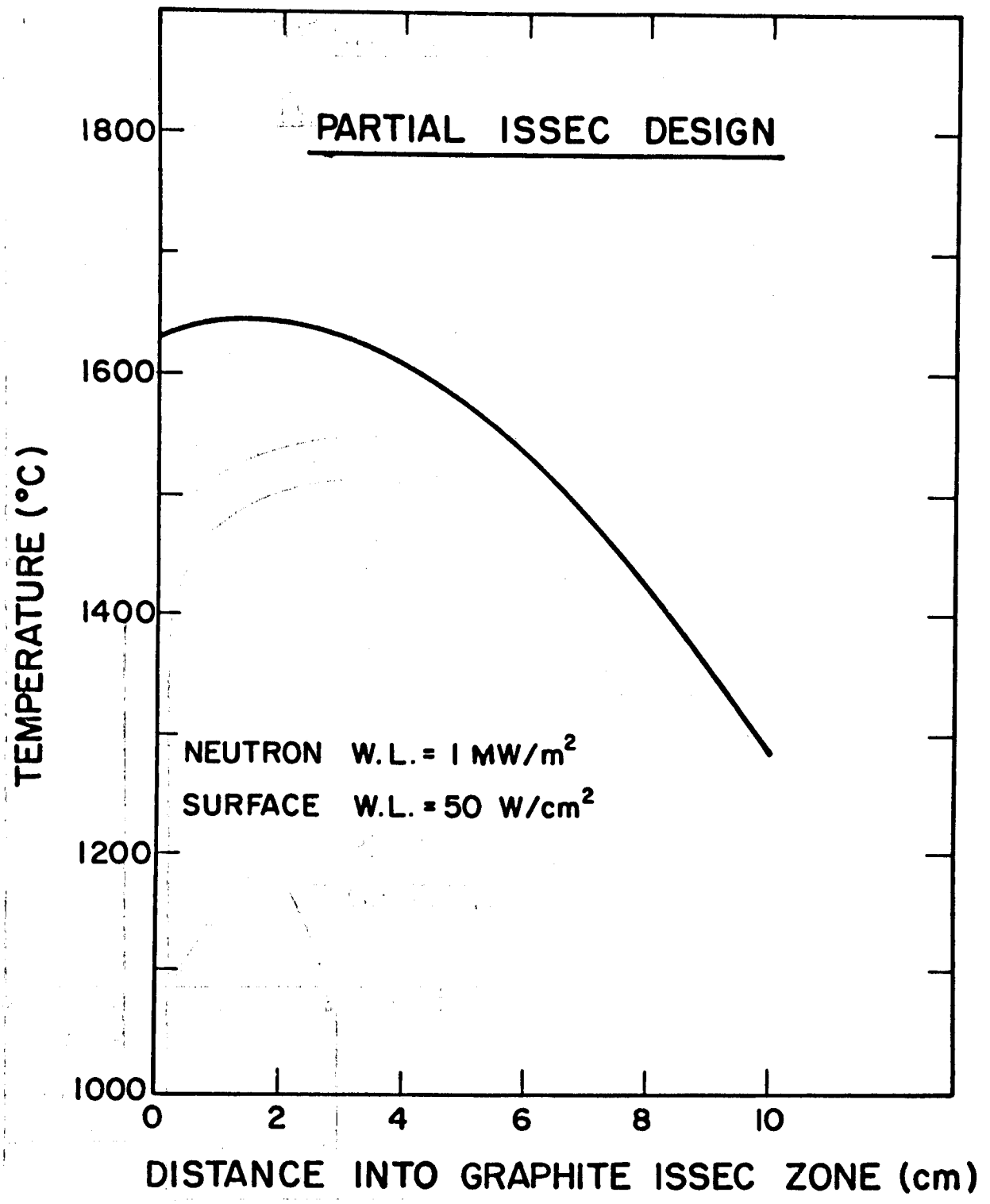
PARTIAL ISSEC DESIGN
1800
1600
1400
1200
1000
TEMPERATURE (°C)
NEUTRON W.L. = 1 MW/m²
SURFACE W.L. = 50 W/cm²
0
2
4
6
8
10
DISTANCE INTO GRAPHITE ISSEC ZONE (cm)

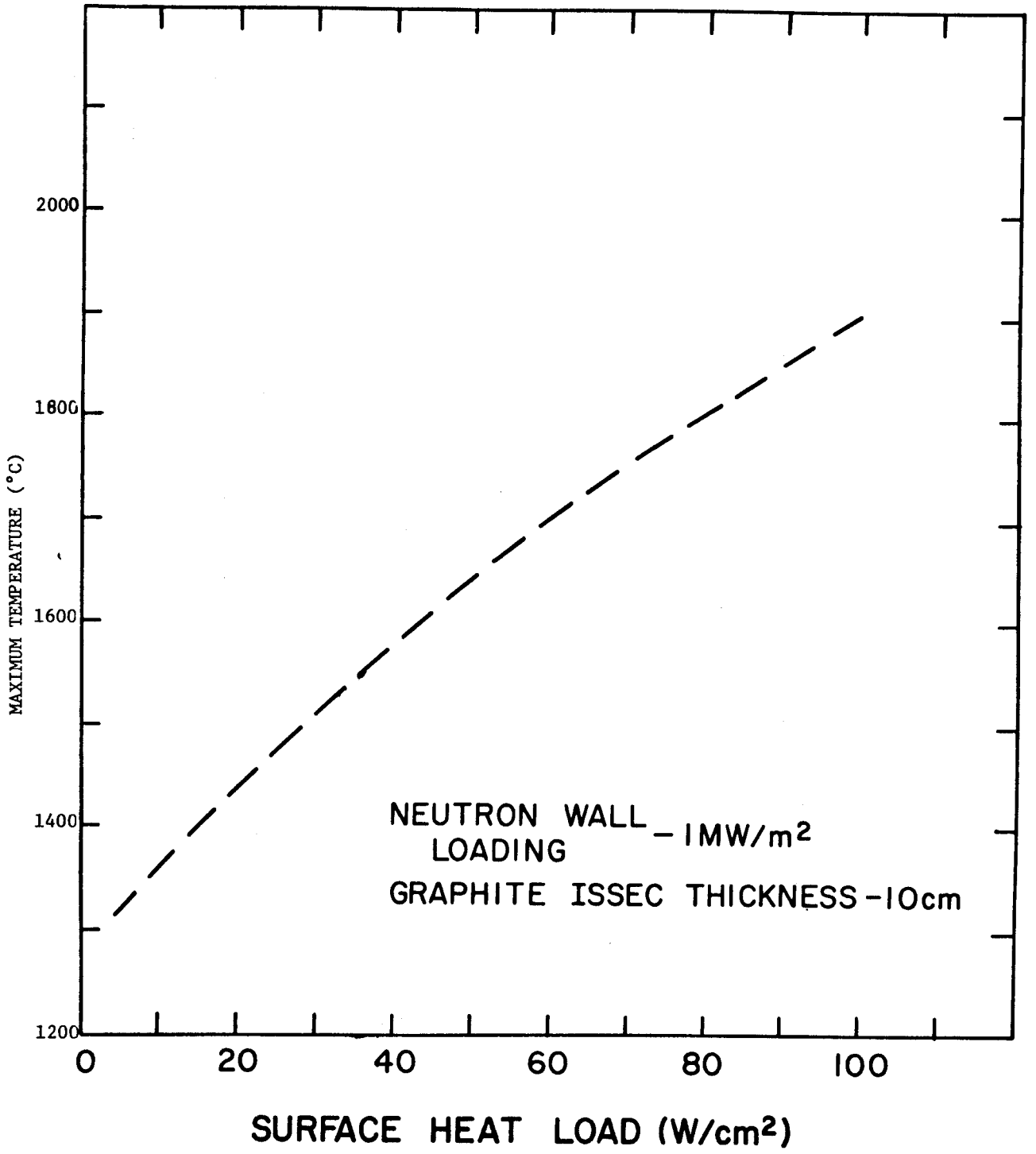
MAXIMUM TEMPERATURE (°C)
2000
1800
1600
1400
1200
0
20
40
60
80
100
SURFACE HEAT LOAD (W/cm²)
NEUTRON WALL LOADING - 1MW/m²
GRAPHITE ISSEC THICKNESS - 10cm

IMPACT OF ALTERNATE ASSUMPTIONS ON MAGNETIC FIELD OR NONCIRCULARITY

SYSTEM	B_T^{max} (kG)	B_T° (kG)	PLASMA RADIUS, a (cm)	$\frac{b}{a}$	I_P (MA)	FIRST WALL AREA (m^2)	14 MeV WALL LOADING (MW/m^2)
BASE CASE	80	38	55	2	2.4	149	0.96
VARIATION #1	80	38	55	3	4.15	195	3.4
VARIATION #2	90	43	55	2	2.7	149	1.54
VARIATION #3	150	71	55	2	4.5	149	11.0
VARIATION #4	150	66	79	1	2.5	130	3.3